Simultaneous structure and carrier tuning of dimorphic clathrate Ba_8Ga_<16>Sn_<30>

PHYSICAL REVIEW B **77**, 235119 (2008)

Simultaneous structure and carrier tuning of dimorphic clathrate $Ba_8Ga_{16}Sn_{30}$

K. Suekuni,[1] M. A. Avila,[1] K. Umeo,[2] H. Fukuoka,[3] S. Yamanaka,[3] T. Nakagawa,[1] and T. Takabatake[1,4]
[1]*Department of Quantum Matter, ADSM, Hiroshima University, Higashi-Hiroshima 739-8530, Japan*
[2]*Cryogenics and Instrumental Analysis Division, N-BARD, Hiroshima University, Higashi-Hiroshima 739-8526, Japan*
[3]*Department of Applied Chemistry, Graduate School of Engineering, Hiroshima University, Higashi-Hiroshima 739-8527, Japan*
[4]*Institute for Advanced Materials Research, Hiroshima University, Higashi-Hiroshima 739-8530, Japan*
(Received 12 March 2008; published 25 June 2008)

We report structural, transport, and thermal properties of carrier-tuned $Ba_8Ga_{16}Sn_{30}$ single crystals with the type-1 clathrate structure (β phase), demonstrating that $Ba_8Ga_{16}Sn_{30}$ is a unique thermoelectric clathrate material wherein both the structure type and the carrier type are tunable. The results are compared with the properties of the better known type-8 structure (α phase) and of $A_8Ga_{16}Ge_{30}$ (A=Sr, Eu). Differential thermal analysis and powder x-ray diffraction show that both phases are stable up to their virtually identical melting point of 520 ± 3 °C. Refinements of single-crystal x-ray diffraction data indicate that the Ba(2) guest ion in the tetrakaidecahedron occupies the off-center 24k sites which are 0.43–0.44 Å away from the centered 6d site. The temperature-linear coefficient of the specific heat is 29 mJ/mol K^2 for both n- and p-type carriers in the β phase, four times larger than that for the α phase, suggesting contributions from tunneling of the Ba(2) guest ions between off-center minima. Analysis of specific heat with a soft-potential model (SPM) gives a characteristic energy of 20 K for the Ba(2) vibration, significantly lower than 50 K for the α phase and in fact the lowest among type-1 clathrates. The lattice thermal conductivities κ_L for the β phase with both charge carrier types are very similar and show a glasslike temperature dependence. This behavior in $\kappa_L(T)$ is also described using SPM analysis, where it is found that the coupling strength between guest modes and acoustic phonons for the β phase is significantly larger than that for $Sr_8Ga_{16}Ge_{30}$.

DOI: 10.1103/PhysRevB.77.235119 PACS number(s): 72.15.Jf, 72.20.Pa, 82.75.−z

I. INTRODUCTION

Intermetallic clathrates are among the very few classes of materials displaying phonon-glass, electron-crystal characteristic and, therefore, under intense investigation as potential candidates for thermoelectric conversion applications.[1–3] Intermetallic clathrates are cage compounds that typically crystallize in type-1, 2, 3, and 8 clathrate structures, with general formulas A_8X_{46}, $A_{24}X_{136}$, $A_{24}X_{100}$, and A_8X_{46}, respectively. All structures are composed of a framework of cage atoms X (usually the group 14 elements Si, Ge, and Sn) which encapsulate guest atoms A. For A_8X_{46} and its subgroup $A_8E_{16}X_{30}$, most compounds are reported in the type-1 structure, such as Ba_8Si_{46},[4] $Eu_8Ga_{16}Ge_{30}$ (EGG),[2,3,5–8] $Sr_8Ga_{16}Ge_{30}$ (SGG),[1,2,9–11] $Ba_8Ga_{16}Ge_{30}$ (BGG).[2,12,13] The type-1 cubic structure ($Pm\bar{3}n$, No. 223) consists of six tetrakaidecahedra and two dodecahedra as shown in Fig. 1(b). In contrast, only EGG and $Ba_8Ga_{16}Sn_{30}$ (BGS) are known so far to form the type-8 structure, also cubic ($I\bar{4}3m$, No. 217) and consisting of eight distorted dodecahedra as shown in Fig. 1(a).[3,14,15] Most clathrates follow the Zintl rule where the cage atoms are partially substituted by acceptor atoms for charge compensation between guest and cage. Owing to the charge compensation, Zintl compounds show large thermopower, therefore attracting attention as potential thermoelectric materials[16,17] and clathrate compounds even more so, especially because of their low lattice thermal conductivity κ_L.[1,2]

It is known that $\kappa_L(T)$ can behave quite differently depending on the charge carrier type (electrons or holes) and the structure type in certain rare cases among clathrate compounds. The carrier types have been found tunable only in Ba-based clathrates such as type-8 BGS, type-1 BGG, and type-1 $Ba_8Ni_{6-x}Ge_{40+x}$.[12,13,18] With increasing temperature, the $\kappa_L(T)$ of n-type samples increases toward a peak as a typical crystal, while the $\kappa_L(T)$ of p-type samples remains at a plateau as a disordered crystal; and the origin of this anomalous behavior remains an open question. Structural tuning is even rarer: the structural dimorphism shown by EGG (type 8: α phase; type 1: β phase) had been a unique case until recently. For α-EGG, all Eu atoms are essentially centered (8c site) in the distorted dodecahedron. In contrast, the Eu(2) atom in β-EGG is located at one of four equivalent positions 24k, which is 0.4 Å away from the cage center position 6d in the tetrakaidecahedron.[5] Interestingly, $\kappa_L(T)$

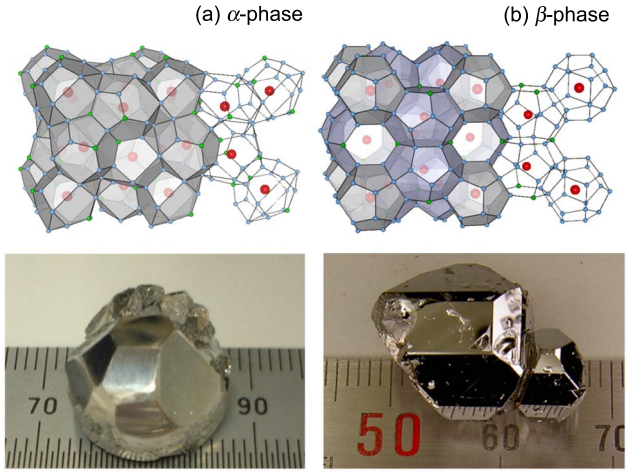

FIG. 1. (Color online) Crystal structures and corresponding as-grown single crystals of (a) α-$Ba_8Ga_{16}Sn_{30}$ and (b) β-$Ba_8Ga_{16}Sn_{30}$.

TABLE I. Starting composition, crystal composition, lattice parameter a, electrical resistivity ρ, thermopower S, and carrier density n at 280 K for α- and β-$Ba_8Ga_{16}Sn_{30}$.

Sample	Starting composition			Crystal composition			Lattice parameter	Electrical resistivity	Thermopower	Carrier density
	Ba	Ga	Sn	Ba	Ga	Sn	a (Å)	ρ (mΩ cm)	S (μV/K)	n (10^{19} cm^{-3})
α phase										
α *n*1	8	16	60	8.0(1)	16.0(2)	30.0(2)	11.585 (1)	4.2	−180	3.8
α *n*2	8	16	60	8.1(1)	15.9(2)	30.1(2)	11.584 (1)	3.2	−110	3.4
α *p*1	8	50	30	8.1(1)	16.1(2)	29.9(2)	11.587 (1)	6.0	150	28
α *p*2	8	40	30	8.0(1)	16.1(2)	29.9(2)	11.589 (1)	39	340	3.5
β phase										
β *n*1	8	16	60	8.0(1)	15.9(2)	30.1(2)	11.685 (1)	40	−300	3.2
β *n*2	8	24	68	7.9(1)	15.8(2)	30.2(2)	11.685 (1)	33	−210	1.0
β *p*1	8	32	60	7.8(1)	15.8(2)	30.2(2)	11.707 (1)	18	220	0.85
β *p*2	8	32	60	8.0(1)	15.8(2)	30.2(2)	11.708 (1)	38	270	0.55

for β-EGG is strongly suppressed in comparison with that for α-EGG and behaves like a typical glass. A previous indication that BGS could also show structural dimorphism[19] has been recently confirmed; in addition, an extremely low κ_L was found for the "new" type-1 morph β-BGS.[20] X-ray diffraction analysis of *n*-type samples revealed that the Ba atom in the tetrakaidecahedron is located at a 24*k* site (0.2437, 0.5, −0.03656) that is 0.43 Å away from the 6*d* site (0.25, 0.5, 0).[20] The off-center displacement is therefore essentially the same as Eu in β-EGG with the glasslike $\kappa_L(T)$. Because the κ_L for β-BGS is also the lowest among ternary type-1 clathrate compounds, it has been suggested that the guest off-center motion is the primary factor responsible for the suppression of κ_L. However, it remained to be seen whether β-BGS could also be carrier-tuned like the other Ba clathrates and what would be the effect of *p*-type cages on the thermoelectric properties.

In this work we report a complete structural, transport, and thermal properties study of *n*- and *p*-type β-BGS single crystals, comparing them with those of the α-phase BGS and $A_8Ga_{16}Ge_{30}$ (A=Sr, Eu). In addition, the nonmagnetic nature of BGS (unlike EGG with an effective magnetic moment of $7.94\mu_B$ for the Eu^{2+} guest ions) enables us to resolve the effect of off-center motion on the thermal conductivity and specific heat. We end by focusing on the general relationship between the guest free space and κ_L of the type-1 clathrates and discussing their potential for thermoelectric conversion applications.

II. CRYSTAL GROWTH AND STRUCTURAL ANALYSIS

The growth and characterization procedures of large polyhedral single crystals (up to 1 cm^3) of α- and β-BGS (Fig. 1) have been described in our previous papers.[15,20] The basic approach is to grow crystals with a self-flux method using excess Ga or Sn, depending on the desired carrier type. High-purity elements are mixed in a glove box, sealed in an evacuated quartz tube, soaked at 490 °C, and slowly cooled over 100 h to 390 °C. The starting batch compositions of the eight samples used in this work are listed in Table I, together with the resulting crystal compositions as determined by electron probe microanalysis on a JEOL JXA-8200 analyzer. As expected, all crystals have almost the same composition of Ba:Ga:Sn=8:16:30, but, especially for the β-phase, the compositions tend to have excess Sn. Our preliminary exploration of the ternary diagram indicates that the β-phase structure is favored by growth in double flux (Ga+Sn) and the carrier type can be simultaneously tuned by adjusting the Ga/Sn ratio. Other factors such as higher temperatures (soaking at 900 °C, cooling between 600 and 400 °C) and shorter cooling times (<100 h) also appear to favor the β-phase growth. However, some attempts to grow crystals in one phase do result in the other, and full control over the growth process will require a more detailed investigation of this ternary system's phase diagram. Differential thermal analysis was performed on crystals of both structures with a Setaram DTA-92–16.18. No indication of phase transitions was observed up to their virtually identical melting points of 520±3 °C, as is shown in Fig. 2.

The crystal structure and lattice parameters of all batches were refined using powder x-ray diffraction (PXRD) on crushed crystals, measured on a MAC Science MX-Labo diffractometer with Cu $K\alpha$ radiation. We notice in Table I that the lattice parameters of the β phase (11.685–11.708 Å) are larger than those of the α phase (11.584–11.589 Å). It is

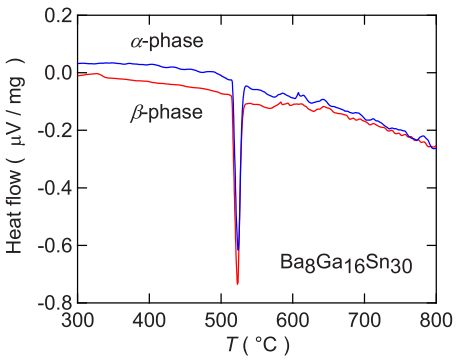

FIG. 2. (Color online) Differential thermal analysis curves obtained on heating at a rate of 5 °C/min for α- and β-$Ba_8Ga_{16}Sn_{30}$.

TABLE II. Atomic coordinates, isotropic displacement parameters U_{eq}, and occupational parameters at 300 K for β-$Ba_8Ga_{16}Sn_{30}$ crystals; β $n1$ (a) and β $p1$ (b), obtained from single-crystal x-ray diffraction analysis.

Atom	Site	x	y	z	U_{eq} (Å^2)	Occupational parameters
			(a)			
Ba(1)	2a	0	0	0	0.0202(1)	1
Ba(2)	24k	0.2437(4)	1/2	−0.03656(16)	0.0524(5)	0.25
Ga(1)/Sn(1)	6c	1/4	0	1/2	0.0181(2)	0.707 (4)/0.293(4)
Ga(2)/Sn(2)	16i	0.18435(2)	0.18435(2)	0.18435(2)	0.0178(1)	0.356(3)/0.644(3)
Ga(3)/Sn(3)	24k	0	0.31227(2)	0.11871(2)	0.0169(1)	0.252(2)/0.748(2)
			(b)			
Ba(1)	2a	0	0	0	0.0220(1)	1
Ba(2)	24k	0.2430(4)	1/2	−0.03685(15)	0.0540(5)	0.25
Ga(1)/Sn(1)	6c	1/4	0	1/2	0.0206(2)	0.675(4)/0.325(4)
Ga(2)/Sn(2)	16i	0.18412(2)	0.18412(2)	0.18412(2)	0.0195(1)	0.338(2)/0.662(2)
Ga(3)/Sn(3)	24k	0	0.31235(2)	0.11848(2)	0.0191(1)	0.264(2)/0.736(2)

interesting to note that there is a very small but consistent increase in the lattice parameters of the p-type samples, which was also reported in BGG.[21] Single crystal x-ray diffraction analysis was performed on selected crystals on a Rigaku R-AXIS diffractometer with an imaging plate area detector using monochromated Mo $K\alpha$ radiation. The structure was solved and refined using the Rigaku CRYSTALSTRUCTURE crystallographic software package.[22] Refined atomic coordinates, occupancies, and isotropic displacement parameters of two samples β $n1$ and β $p1$ with n- and p-type carriers, respectively, are summarized in Table II (a and b), respectively. The lattice parameters and the unit cell volumes are $a=11.685(3)$ Å, $V=1595.5(7)$ Å^3 for β $n1$ and $a=11.708(1)$ Å, $V=1604.8(2)$ Å^3 for β $p1$, in good agreement with the results of PXRD. The final values of the reliability factors R (R_w) are 0.0097 (0.0110) and 0.0103 (0.0137) for β $n1$ and β $p1$, respectively. Such low values for a complex and disordered system evidence the good crystallinity of the samples and the validity of the structural model, allowing further detailed analysis. Unlike Ga-Ge clathrates, the x-ray atomic scattering factor difference between Ga and Sn atoms allows enough contrast to resolve site occupation preferences. Ga atoms were found to preferentially occupy the 6c site in both crystals (about 71% and 68%, respectively) consistent with the reported structural analyses for $Ba_8Ga_{16}Ge_{30}$ using synchrotron x-ray diffraction and high-resolution neutron diffraction.[21] By occupying the 6c site, the number of Ga-Ga bonds, which require higher energy and tend to cause lattice distortion due to electrostatic repulsion, is minimized. Although many early works on type-1 clathrates treated the framework as having a random distribution of atoms,[23] this type of preferential occupation now seems to be well accepted as a ubiquitous feature of the type-1 structure.[21,24,25]

For β $n1$ and β $p1$ samples, the off-center 24k sites of the Ba(2) guest are 0.434(3) and 0.439(2) Å away from the centered 6d site, respectively. There is little difference between n- and p-type crystals, in accordance with several techniques used so far to study the structure of $Ba_8Ga_{16}X_{30}$ (X =Ge, Sn).[13,21,26,27] With decreasing temperature from 300 to 120 K, the isotropic displacement parameters U_{eq} for all atoms in β $n1$ and that for Ba(2) in β $p1$ linearly decrease, as shown in Fig. 3(a). The temperature dependences of U_{eq} for the guest Ba atom and the framework Ga/Sn atoms are respectively written as

$$U_{eq}(\mathrm{Ba}) = \frac{\hbar^2}{2m_g k_B \theta_E}\coth\left(\frac{\theta_E}{2T}\right) + d^2, \tag{1}$$

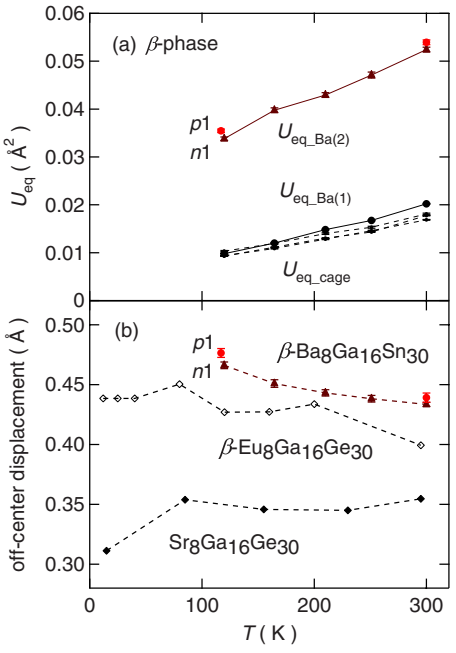

FIG. 3. (Color online) (a) Temperature dependence of isotropic displacement parameters U_{eq} of Ba(2) for $n1$ and $p1$, Ba(1) and cage atoms for $n1$ in β-$Ba_8Ga_{16}Sn_{30}$. (b) Temperature dependence of off-center displacement d_{6d-24k} of Ba(2) atom in β-$Ba_8Ga_{16}Sn_{30}$, Eu(2) atom in β-$Eu_8Ga_{16}Ge_{30}$, and Sr(2) atom in $Sr_8Ga_{16}Ge_{30}$ (Refs. 5 and 9).

$$U_{\mathrm{eq}}(\mathrm{Ga/Sn}) = \frac{3\hbar^2 T}{m_{\mathrm{av}} k_B \theta_D^2}\left[\frac{T}{\theta_D}\int_0^{\theta_D/T}\frac{x}{\exp(x)-1}dx + \frac{\theta_D}{4T}\right] + d^2, \tag{2}$$

where m_g, m_{av}, and d^2 are mass of the guest atom (Ba), the average mass of the framework atoms (Ga/Sn), and temperature-independent disorder term, respectively.[25] For the β $n1$ sample, the fits with these equations yield the characteristic temperatures $\theta_{\mathrm{EH}}=78$ K for Ba(1) and $\theta_{\mathrm{EL}}=60$ K for Ba(2) and the Debye temperature of the cage $\theta_D=194-203$ K. Comparable Debye temperatures of 207 K (218 K) for α phase (β phase) were also calculated independently from the sound velocities $v_{(C11)}=2850$ (3369) m/s, $v_{(C11-C12)/2}=1950$ (1936) m/s, and $v_{(C44)}=1950$ (1844) m/s obtained by ultrasound measurements at 4 K.[32] In contrast, the off-center displacement d_{6d-24k} of Ba(2) seems to slightly *increase* with decreasing temperature from 300 to 120 K [Fig. 3(b)], even though the lattice parameter contracts by 0.19%. As the thermal energy of the atoms is lost on cooling, the attraction of the Ba(2) ion toward the nearest cage atom may become more effective[28] so that its off-center displacement increases. By plotting in Fig. 3(b) the off-center displacements of the Eu atom in β-EGG and Sr atom in SGG,[5,9] one notices similar behaviors between β-BGS and β-EGG, but apparently not for SGG.[29] The level of ion-to-cage size mismatch may therefore play an important role in this behavior.

III. THERMAL AND TRANSPORT MEASUREMENTS AND DISCUSSIONS

Electrical resistivity ρ and thermopower S were measured in homemade systems by standard dc four-probe method and a differential method, respectively, in the temperature range from 4 to 300 K. The Hall coefficient R_H was measured by a dc method in a field of 1 T applied by a conventional electromagnet. Thermal conductivity κ was measured using a steady-state method in ^{3}He and ^{4}He cryostats in the ranges of 0.3–5.0 K and 4.2–300 K, respectively. The data sets overlap well in the intermediate range between 4.2 and 5 K. The data of κ is reliable up to about 150 K, above which the effect of thermal losses by wire conduction and radiation requires corrections. The specific heat from 0.3 to 200 K was measured on a Quantum Design physical property measurement system using its standard thermal-relaxation method.

The $\rho(T)$ and $S(T)$ for eight α- and β-phase samples are displayed in Fig. 4. The sign of S agrees with that of R_H, which depends on the type of dominant charge carriers. The carrier density calculated from $n=1/eR_H$ at 280 K is listed in Table I. The absolute values of S sublinearly increase to 100–300 μV/K with increasing temperature. The $\rho(T)$ exhibits behaviors of a low carrier density metal or a heavily doped semiconductor. The values of ρ for the β-phase samples are typically larger than the α-phase ones, consistent with the fact that the carrier densities n for the β-phase samples are smaller than those for the α-phase samples (see Table I). This may reflect that the semiconducting band gap is larger in the β phase.[30] Since the sample composition and fine structural details can be growth-technique dependent,[24] it remains to be examined whether other methods or flux growth optimization can successfully synthesize β-phase samples with higher carrier densities.

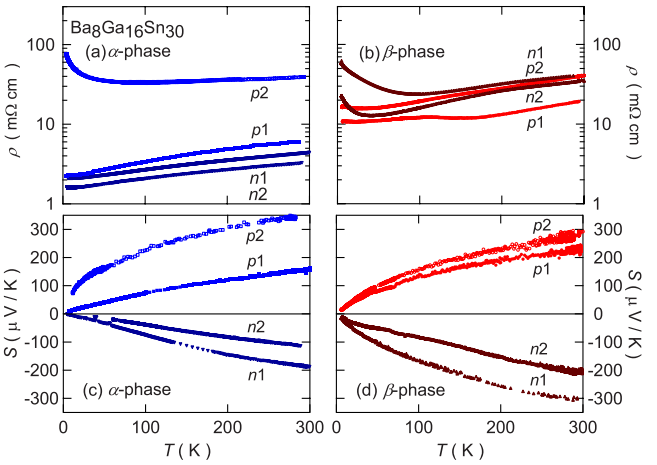

FIG. 4. (Color online) Temperature dependence of electrical resistivity ρ for (a) α-$Ba_8Ga_{16}Sn_{30}$ and (b) β-$Ba_8Ga_{16}Sn_{30}$. The corresponding temperature dependences of thermopowers S are plotted in (c) and (d), respectively. The color and symbol scheme for all samples shown here is maintained consistent throughout subsequent figures.

To complement the structural and transport data, a great deal of useful information can be extracted from specific heat measurements. We initially focus on the lowest temperature range of the specific heat, plotted in a C/T vs T^2 graph [Fig. 5(a)]. At first glance, the linear behaviors of all four sets of data below 1 K might suggest that they can be well described by the conventional expression $C/T=A+BT^2$, with a temperature-linear coefficient A and a Debye coefficient B. However, closer inspection leads to a different conclusion. Linear fits for the α $n2$ and α $p2$ samples (solid lines) yielded A coefficients of 7.2 and 9.4 mJ/mol K^2, in good agreement with the Sommerfeld coefficient γ of 7 mJ/mol K^2, which is expected by the free electron model for a sample with carrier density 1×10^{20} cm^{-3}.[15] In contrast, for the β $p1$ sample the A coefficient of 29 mJ/mol K^2 is a factor of 10 times larger than the expected γ value of 3 mJ/mol K^2 from a carrier density of 1×10^{19} cm^{-3}. This discrepancy is indicative of extra entropy at low temperatures, most likely arising from the tunneling of the guest ions among the off-center split sites. The idea is supported by the observation that the T-linear coefficient in β-EGG with off-center split sites is eight times larger than that for α-EGG with on-center site.[7] The low-temperature contribution of tunneling states in glasses is known to behave as $C=DT$,[31] and as such convolutes with the T-linear term of the electronic contribution. Therefore, γ and D cannot be easily deconvoluted from the measured coefficient A, but the difference by a factor of 10 in the β phase allows us to ignore the electronic contribution in the subsequent analysis. Also note the very different slopes B between the α and β phases, inconsistent with the very similar Debye temperatures obtained in Sec. II.

We now direct our attention to the intermediate temperature range and plot the data as C/T^3 vs T in Fig. 5(b). The

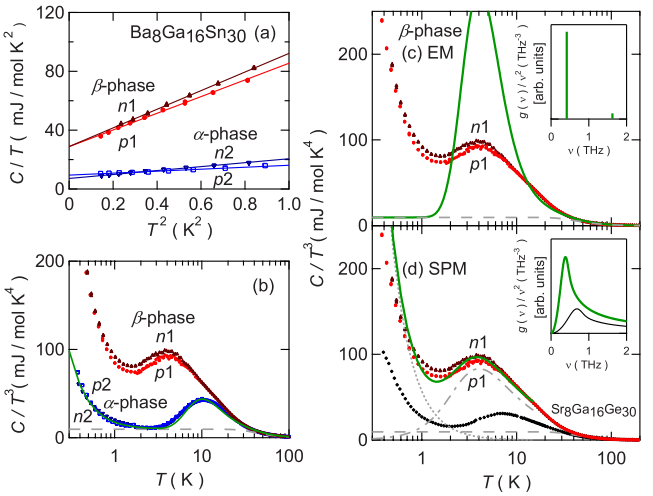

FIG. 5. (Color online) (a) Temperature dependence of specific heat presented as C/T vs T^2 for α- and β-$Ba_8Ga_{16}Sn_{30}$. The solid lines are fits with the relation $C/T=A+BT^2$. (b) Temperature dependence of specific heat presented as C/T^3 vs T for α- and β-$Ba_8Ga_{16}Sn_{30}$. The solid line for the α-phase data is the sum of Einstein contribution C_E with $\theta_E=50$ K, Debye contribution C_D with $\theta_D=210$ K (dashed line), and electronic contribution C_{el} with $\gamma=8$ mJ/mol K^2. (c) and (d) The specific heat presented as C/T^3 vs T for the n- and p-type β-$Ba_8Ga_{16}Sn_{30}$ and $Sr_8Ga_{16}Ge_{30}$ (diamonds) (Ref. 10) and fit to the data with two models; (c) EM and (d) SPM. The solid line in (c) is the sum of two Einstein contributions $C_{EL}+C_{EH}$ and the Debye contributions C_D. The solid line in (d) is the sum of the soft modes C_{SM} (dashed-dotted line), the tunneling two level system C_{TLS} (dotted line), and the Debye contribution C_D with $\theta_D=210$ K (dashed line). The insets show the vibrational density of states $g(\nu)/\nu^2$ for β-BGS (thick line) and SGG (thin line) as a function of the frequency ν for the EM and SPM.

most significant observation is the large and broad peak for the β phase. The peak temperature of 4 K is lower than 10 K for the α phase, which implies a lower characteristic guest vibration energy. We recall here that (unlike EGG) no magnetic freedoms are present to contribute in this system and, therefore, this major enhancement in C/T^3 for the β phase clearly arises from the Ba guest vibrational entropy. For quantitative analysis and to minimize the fitting parameters, first we assume that the framework composed of $(Ga,Sn)_{46}$ cages is a stiff Debye solid. The very similar θ_D for both structure types obtained in Sec. II confirm that the cage vibrations have no direct contribution to the enhanced C/T of the β phase observed in Fig. 5(a). For simplicity, a Debye term in specific heat C_D of $\theta_D=210$ K is fixed in all subsequent fittings. This contribution is shown as a dashed line in Fig. 5, and its line thickness is comparable to the uncertainty range for $\theta_D=207-218$ K. It provides a good baseline on which the Einstein contribution from Ba ions appears in the α phase. Indeed, the behavior of the eight equal Ba ions is satisfactorily described using the Einstein model (EM) of independent harmonic oscillators, with $\theta_E=50$ K [see Fig. 5(b)]. For type-1 clathrates, the analysis becomes somewhat more complex. At least two Einstein temperatures θ_{EL} and θ_{EH} are required to describe the anisotropic guest vibrations in the six tetrakaidecahedrons (in-plane and out-of-plane vibrations, respectively) plus an additional Einstein temperature for the isotropic guest vibration in the two dodecahedrons. To minimize fitting parameters, we make the reasonable approximation that this last term is the same as θ_{EH} and keep the numbers of Einstein oscillators fixed at six and two. This model works well for analysis of the $C(T)$ for various type-1 clathrates wherein the guest ion is only slightly off-center, such as $Sr_8Ga_{16}Si_{30}$ and BGG,[11,13] in which anharmonic contributions can be regarded as a small perturbation over the harmonic vibration. When applied to sample β $n1$, with three terms C_D using $\theta_D=210$ K from the sound velocity, C_{EH} using $\theta_{EH}=78$ K from the structural analysis, and C_{EL} using $\theta_{EL}=20$ K, this model proves completely inadequate [Fig. 5(c)] because of the strong anharmonicity of the guest vibration.

A better description of $C(T)$ for the β phase may be given by the soft-potential model (SPM) which could reproduce well the broad peak of C/T^3 for SGG.[10] This model was originally developed to describe the anomalous properties of glasses such as an extended vibrational density of states. According to the SPM,[33] the potential of the soft modes (SM) is given by

$$V(x) = W(D_1x + D_2x^2 + x^4), \tag{3}$$

where x is the dimensionless displacement of the vibrating unit, D_1 and D_2 are the coefficients of the asymmetry and harmonic-potential terms which vary from mode to mode, and W is the characteristic energy of the potential. The coefficients D_1 and D_2 can be either positive or negative. The distribution function $P(D_1,D_2)$ is assumed to be Gaussian with respect to D_1, which is centered around zero, and it is independent of D_2; that is,

$$P(D_1,D_2) = P_s \exp(-AD_1^2), \tag{4}$$

where A and P_s are the distribution broadness of the soft vibrational mode and distribution constant of the SM, respectively.[34] The soft vibrational density of states g as a function of the frequency ν is described by

$$g(\nu) = \frac{1}{8}\frac{P_s}{W}\left(\frac{h\nu}{W}\right)^4 \int_0^1 \exp\left[-A\left(\frac{h\nu}{2W}\right)^6 t^2(1-t^2)^2\right]dt. \tag{5}$$

The contribution of SM to the specific heat C_{SM} can then be evaluated simply as

$$C_{SM} = \int_0^\infty g(\nu)C_h(x)d\nu, \tag{6}$$

where the specific heat of a single harmonic oscillator C_h is given by

$$C_h(x) = k_B\frac{x^2e^{-x}}{(1-e^{-x})^2}, \quad x = \frac{\hbar\omega}{k_BT}. \tag{7}$$

Additionally, the contribution of tunneling two level systems (TLS) to the specific heat is described approximately as

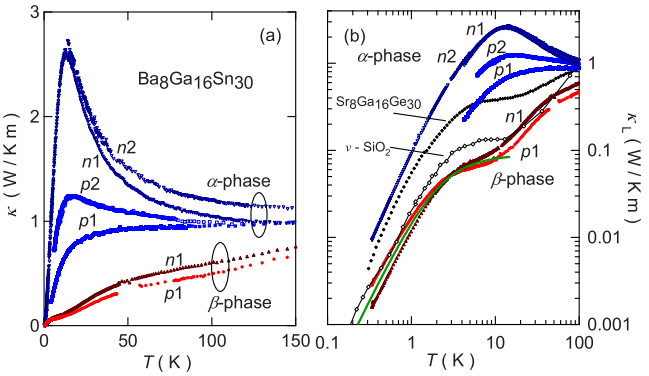

FIG. 6. (Color online) (a) Temperature dependence of thermal conductivity κ for α- and β-$Ba_8Ga_{16}Sn_{30}$. (b) Temperature dependence of lattice thermal conductivity κ_L for n- and p-type α- and β-$Ba_8Ga_{16}Sn_{30}$, $Sr_8Ga_{16}Ge_{30}$ (closed diamonds) (Ref. 10) and vitreous SiO_2 (open diamonds) (Ref. 35). The solid line is the fit to the data of β-$Ba_8Ga_{16}Sn_{30}$ sample by using the soft-potential model (see text).

$$C_{\mathrm{TLS}} \cong \frac{\pi^2}{6}\left(\frac{1}{9}\right)^{1/3}\frac{P_s}{W}k_B^2 T \ln^{1/3}\left[\frac{t_{\mathrm{exp}}}{\tau_{\mathrm{min}}(k_B T)}\right], \tag{8}$$

where t_{exp} and τ_{min} are a typical experimental time and the minimum relaxation time of tunneling states, respectively. We have set $t_{\mathrm{exp}}=10$ s and $\tau_{\mathrm{min}}=1\times10^{-9}$ T^{-3}, as in the case of SGG.[10] To reproduce both the position and height of the peak in C/T^3, other parameters are chosen as $A=0.017$, $W/k_B=3.5$ K, and $P_s=6.4\times10^{21}$ mol^{-1}. The solid line in Fig. 5(d) is the sum of the three contributions, C_{SM} (dashed-dotted line), C_{TLS} (dotted line), and C_D (dashed line). Note that the broad peak around 4 K and rapid increase below 1 K are the contributions of SM and TLS, respectively. Using the above parameters, the vibrational density of states $g(\nu)$ results, as shown in the inset of Fig. 5(d). The profile of $g(\nu)/\nu^2$ has a broad peak around 0.4 THz, to be compared with the two delta functions implicit in the previous analysis with the Einstein model [see the inset of Fig. 5(c)]. For comparison, $g(\nu)/\nu^2$ of SGG peaking at 0.7 THz and its measured specific heat are represented in Fig. 5(d).[10]

Figure 6(a) displays $\kappa(T)$ for the α- and β-phase BGS samples. For α $n1$ and α $n2$ samples, $\kappa(T)$ shows a typical crystalline peak at 14 K, which is suppressed in the α $p1$ and α $p2$ samples. Therefore, a large influence of the charge carrier type exists in the α phase.[13] In contrast, the β phase shows classic glass-like $\kappa(T)$ for both n- and p-type samples. In this phase, the electronic contribution $\kappa_{\mathrm{el}}(T)$ is much smaller than the lattice contribution $\kappa_L(T)$ due to the low charge carrier densities of 10^{19} cm^{-3}. The large reduction in $\kappa(T)$ is mostly ascribed to the drastic reduction of $\kappa_L(T)=\kappa(T)-\kappa_{\mathrm{el}}(T)$, which can be estimated using the resistivities in Fig. 4 and the Wiedemann–Franz law $\kappa_{\mathrm{el}}(T)=(\pi^2k_B^2/3e^2)T/\rho(T)$. The $\kappa_L(T)$ thus calculated is shown in Fig. 6(b). For the β phase, $\kappa_L(T)$ is significantly lower than those of the α phase and SGG. It is in fact lower than that of vitreous SiO_2,[35] a model glass system, and generally follows its behavior: a T^2 dependence below 1 K, a resonance dip/plateau around 4 K, and roughly T-linear dependence above 10 K (which should eventually cross over to a weak decrease at much higher temperatures).

To help understand the lower temperature glasslike behavior of β-phase BGS, we also analyze the $\kappa_L(T)$ within the framework of the SPM for glassy systems.[33] $\kappa_L(T)$ is expressed as

$$\kappa = \frac{6k_B}{\pi C^*}\left(\frac{W}{h}\right)^2\left(\frac{1}{v_l}+\frac{2}{v_t}\right)\frac{z^2}{1.1+0.7z+3z^2}, \tag{9}$$

where C^* is a dimensionless coupling parameter and v_l and v_t are the longitudinal and transverse sound velocities, respectively, and $z=k_BT/W$.[33] In this model, three scattering mechanisms are concerned: tunneling states, classical activated relaxations, and soft vibrational modes. As a result, the data below 10 K are reproduced well using $W/k_B=3.5$ K obtained by specific heat analysis, sound velocities $v_l=3369$ m/s and $v_t=(1936+1844)/2$ m/s, and $C^*=7.0\times10^{-4}$. The fact that C^* for β-BGS is more than twice that of SGG (2.9×10^{-4}) (Ref. 10) reflects the stronger coupling of the guest modes with sound waves in β-BGS.

IV. GUEST FREE SPACE AND LATTICE THERMAL CONDUCTIVITY

Another interesting issue of the thermal behavior in type-1 clathrates is the intimate relationship between the magnitude of κ_L and the guest free space for vibration. This concept follows the ideas proposed to explain the thermal transport of type-1 clathrates[36] and filled skutterudites.[37–39] The free space for guest vibration in the tetrakaidecahedron can be written as $R_{\mathrm{free}}=R_{\mathrm{cage}}-r_{\mathrm{cage}}-r_{\mathrm{guest}}$, where R_{cage} is the cage radius defined as the distance between the 6d (guest) site and the 24k (cage) site. Here, R_{cage} is estimated as $R_{\mathrm{cage}}(A_8E_{16}X_{30})=R_{\mathrm{cage}}(\mathrm{SGG})\times a(A_8E_{16}X_{30})/a(\mathrm{SGG})$, where the reference values for SGG are $R_{\mathrm{cage}}=4.156$ Å and $a=10.724$ Å.[9] r_{guest} is the ionic radius of the guest in a high coordination environment (Rb: 1.83 Å; Sr: 1.44 Å; Cs:

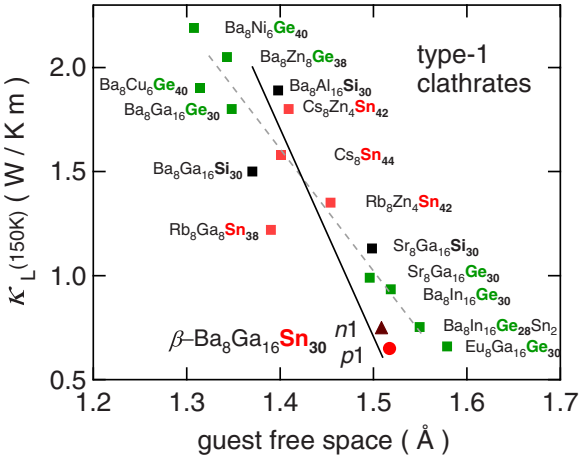

FIG. 7. (Color online) Lattice thermal conductivity κ_L at 150 K vs guest free space in various type-1 clathrates. The solid line is the projected line for Sn clathrates and the dashed line is that for Ge clathrates. The data of κ_L except for β-$Ba_8Ga_{16}Sn_{30}$ are taken from literature (Refs. 7, 11, 13, 18, and 41–45).

1.88 Å; Ba: 1.61 Å; Eu: 1.35 Å)[40] and r_{cage} is the covalent radius of the dominant cage atom (Si: 1.11 Å; Ge: 1.22 Å; Sn: 1.41 Å). For β-BGS $p1$, R_{free} is largest among Sn clathrates, which leads to the lowest κ_L=0.65 W/K m at 150 K. As is shown in Fig. 7, these results accede to a universal inverse relation between R_{free} and κ_L at 150 K in Sn clathrates as well as Ge and Si clathrates.[7,11,13,18,41–45] This relation suggests that phonon scattering is universally enhanced when the guest vibration is characterized by lower energy and larger anharmonicity, at least in the vibrational energy range attained by the known systems. We can therefore regard the relation as a "guideline" for the synthesis of novel compounds with lower κ_L and improve thermoelectric figures of merit. In the case of β-BGS, the value of κ_L is extremely low, but it is still necessary to decrease the electrical resistivity level.

V. CONCLUSIONS

We have reported structural and thermoelectric properties of carrier-tuned β-$Ba_8Ga_{16}Sn_{30}$ and compared them with the better known α phase, demonstrating that this compound is the first clathrate system wherein structure type and carrier type can be simultaneously, and independently, tuned. The crystal structure of the β phase is almost the same for samples with n- and p-type carriers, and the Ba guests occupy split sites that are 0.43–0.44 Å away from the center of the tetrakaidecahedron, the largest displacement among type-1 clathrates. The anomalous low-temperature specific heat of the β-phase could be clearly attributed to the Ba(2) guest vibrational behavior. An upturn and broad maximum in C/T^3 at low temperatures could be reproduced using the soft-potential model of glassy systems, which includes the contributions of tunneling states and soft (quasiharmonic) vibrational modes. The tunneling among split positions is considered responsible for the anomalously large T-linear specific heat coefficient of 29 mJ/mol K^2. A very low characteristic energy of 20 K for the principal soft mode was estimated, significantly lower than that for SGG. Unlike all previous known Ba-based clathrate systems, the κ_L of β-BGS shows classic glasslike temperature dependence irrespective of the charge carrier type and a heat conduction level that is lower than all ternary type-1 clathrates, in fact lower than vitreous SiO_2. The extreme glassy behavior is consistent with an enhanced coupling of the guest tunneling and soft vibrational modes with lattice sound waves in β-BGS. Furthermore, we demonstrate that the β-BGS thermal behavior is consistent with a universal inverse relation between guest free space and the magnitude of κ_L in type-1 clathrates. This relation thus provides a guideline for synthesis of high performance thermoelectric materials which have low levels of κ_L.

ACKNOWLEDGMENTS

We thank P. C. Canfield for valuable suggestions for the preparation of the manuscript and Y. Shibata for the electron probe microanalysis performed at N-BARD, Hiroshima University. Thermal conductivity down to 0.3 K and specific heat were measured at N-BARD, Hiroshima University. This work was financially supported by Grants in Aid for Scientific Research (A) (Grant No. 18204032), the priority area "Nanospace" (Grant No. 19051011) from MEXT, Japan, and the Sasakawa Scientific Research Grant from the Japan Science Society.

[1] G. S. Nolas, J. L. Cohn, G. A. Slack, and S. B. Schujman, Appl. Phys. Lett. **73**, 178 (1998).
[2] B. C. Sales, B. C. Chakoumakos, R. Jin, J. R. Thompson, and D. Mandrus, Phys. Rev. B **63**, 245113 (2001).
[3] S. Paschen, W. Carrillo-Cabrera, A. Bentien, V. H. Tran, M. Baenitz, Yu. Grin, and F. Steglich, Phys. Rev. B **64**, 214404 (2001).
[4] S. Yamanaka, E. Enishi, H. Fukuoka, and M. Yasukawa, Inorg. Chem. **39**, 56 (2000).
[5] B. C. Chakoumakos, B. C. Sales, and D. G. Mandrus, J. Alloys Compd. **322**, 127 (2001).
[6] V. Pacheco, A. Bentien, W. Carrillo-Cabrera, S. Paschen, F. Steglich, and Yu. Grin, Phys. Rev. B **71**, 165205 (2005).
[7] A. Bentien, V. Pacheco, S. Paschen, Yu. Grin, and F. Steglich, Phys. Rev. B **71**, 165206 (2005).
[8] I. Zerec, V. Keppens, M. A. McGuire, D. Mandrus, B. C. Sales, and P. Thalmeier, Phys. Rev. Lett. **92**, 185502 (2004).
[9] B. C. Chakoumakos, B. C. Sales, D. G. Mandrus, and G. S. Nolas, J. Alloys Compd. **296**, 80 (2000).
[10] K. Umeo, M. A. Avila, T. Sakata, K. Suekuni, and T. Takabatake, J. Phys. Soc. Jpn. **74**, 2145 (2005).
[11] K. Suekuni, M. A. Avila, K. Umeo, and T. Takabatake, Phys. Rev. B **75**, 195210 (2007).
[12] A. Bentien, M. Christensen, J. D. Bryan, A. Sanchez, S. Paschen, F. Steglich, G. D. Stucky, and B. B. Iversen, Phys. Rev. B **69**, 045107 (2004).
[13] M. A. Avila, K. Suekuni, K. Umeo, H. Fukuoka, S. Yamanaka, and T. Takabatake, Phys. Rev. B **74**, 125109 (2006).
[14] W. Carrillo-Cabrera, R. Cardoso Gil, V.-H. Tran, and Yu. Grin, Z. Kristallogr. - New Cryst. Struct. **217**, 181 (2002).
[15] D. Huo, T. Sakata, T. Sasakawa, M. A. Avila, M. Tsubota, F. Iga, H. Fukuoka, S. Yamanaka, S. Aoyagi, and T. Takabatake, Phys. Rev. B **71**, 075113 (2005).
[16] X. J. Wang, M. B. Tang, J. T. Zhao, H. H. Chen, and X. X. Yang, Appl. Phys. Lett. **90**, 232107 (2007).
[17] S. R. Brown, S. M. Kauzlarich, F. Gascoin, and G. J. Snyder, Chem. Mater. **18**, 1873 (2006).
[18] A. Bentien, S. Johnsen, and B. B. Iversen, Phys. Rev. B **73**, 094301 (2006).
[19] H. G. von Schnering, W. Carrillo-Cabrera, R. Kröner, E.-M. Peters, and K. Peters, Z. Kristallogr. - New Cryst. Struct. **213**, 679 (1998).
[20] M. A. Avila, K. Suekuni, K. Umeo, H. Fukuoka, S. Yamanaka, and T. Takabatake, Appl. Phys. Lett. **92**, 041901 (2008).
[21] M. Christensen, N. Lock, J. Overgaard, and B. B. Iversen, J. Am. Chem. Soc. **128**, 15657 (2006).

[22] CRYSTALSTRUCTURE3.8, Crystal Structure Analysis Package, Rigaku and MSC, 2000–2006.
[23] B. Eisenmann, H. Schafer, and R. Zagler, J. Less-Common Met. **118**, 43 (1986).
[24] M. Christensen and B. B. Iversen, Chem. Mater. **19**, 4896 (2007).
[25] A. Bentien, E. Nishibori, S. Paschen, and B. B. Iversen, Phys. Rev. B **71**, 144107 (2005).
[26] Y. Takasu, T. Hasegawa, N. Ogita, M. Udagawa, M. A. Avila, K. Suekuni, and T. Takabatake (unpublished).
[27] Y. Jiang, F. Bridges, J. Guzman, G. Kurcvail, M. A. Avila, and T. Takabatake (unpublished).
[28] F. Bridges and L. Downward, Phys. Rev. B **70**, 140201(R) (2004).
[29] R. Baumbach, F. Bridges, L. Downward, D. Cao, P. Chesler, and B. Sales, Phys. Rev. B **71**, 024202 (2005).
[30] Y. Li, J. Gao, N. Chen, Y. Lin, Z. P. Luo, R. H. Zhang, X. Q. Ma, and G. H. Cao, Physica B (Amsterdam) **403**, 1140 (2008).
[31] U. Buchenau, Yu. M. Galperin, V. L. Gurevich, and H. R. Schober, Phys. Rev. B **43**, 5039 (1991).
[32] I. Ishii, T. Fujita, M. A. Avila, K. Suekuni, T. Takabatake, and T. Suzuki (unpublished).
[33] M. A. Ramos and U. Buchenau, in *Tunneling Systems in Amorphous and Crystalline Solids*, edited by P. Esquinazi (Springer, Berlin, 1998), Chap. 9, p. 527.
[34] A. Lindqvist, O. Yamamuro, I. Tsukushi, and T. Matsuo, J. Chem. Phys. **107**, 5103 (1997).
[35] R. C. Zeller and R. O. Pohl, Phys. Rev. B **4**, 2029 (1971).
[36] G. S. Nolas, G. A. Slack, and S. B. Schujman, in *Semiconductors and Semimetals*, edited by T. M. Tritt (Academic, New York, 2000), Vol. 69, p. 255.
[37] L. D. Chen, Proceedings of the 21st International Conference on Thermoelectrics, IEEE, 2002, p. 42.
[38] T. Takabatake, E. Matuoka, S. Narazu, H. Hayashi, S. Morimoto, T. Sasakawa, K. Umeo, and M. Sera, Physica B (Amsterdam) **383**, 93 (2006).
[39] C. Uher, in *Semiconductors and Semimetals*, edited by T. M. Tritt (Academic, New York, 2000), Vol. 69, p. 139.
[40] R. D. Shannon, Acta Crystallogr., Sect. A: Cryst. Phys., Diffr., Theor. Gen. Crystallogr. **32**, 751 (1976).
[41] J. L. Cohn, G. S. Nolas, V. Fessatidis, T. H. Metcalf, and G. A. Slack, Phys. Rev. Lett. **82**, 779 (1999).
[42] G. S. Nolas, J. L. Cohn, J. S. Dyck, C. Uher, and J. Yang, Phys. Rev. B **65**, 165201 (2002).
[43] N. Melnychenko-Koblyuk, A. Grytsiv, L. Fornasari, H. Kaldarar, H. Michor, F. Röhrbacher, M. Koza, E. Royanian, E. Bauer, P. Rogl, M. Rotter, H. Schmid, F. Marabelli, A. Devishvili, M. Doerr, and G. Giester, J. Phys.: Condens. Matter **19**, 216223 (2007).
[44] C. L. Condron, J. Martin, G. S. Nolas, P. M. B. Piccoli, A. J. Schultz, and S. M. Kauzlarich, Inorg. Chem. **45**, 9381 (2006).
[45] K. Suekuni, M. A. Avila, K. Umeo, and T. Takabatake, J. Phys. Soc. Jpn. **77**, Suppl A. 61 (2008).